1993 NASA/ASEE SUMMER FACULTY FELLOWSHIP PROGRAM

JOHN F. KENNEDY SPACE CENTER
UNIVERSITY OF CENTRAL FLORIDA

MASS PROPERTIES MEASUREMENT SYSTEM: DYNAMICS AND STATICS MEASUREMENTS

PREPARED BY:	Dr. Keith L. Doty
ACADEMIC RANK:	Professor
UNIVERSITY AND DEPARTMENT:	University of Florida Department of Electrical Engineering
NASA/KSC	
DIVISION:	Mechanical Engineering
BRANCH:	Special Projects
NASA COLLEAGUE:	Bill Jones Todd Graham
DATE:	August 7, 1993
CONTRACT NUMBER:	University of Central Florida NASA-NGT-60002 Supplement: 11

TABLE OF CONTENTS

ABSTRACT

This report presents and interprets experimental data obtained from the Mass Properties Measurement System (MPMS). Statics measurements yield the center-of-gravity of an unknown mass and dynamics measurements yield its inertia matrix. Observations of the MPMS performance has lead us to specific design criteria and an understanding of MPMS limitations.

ACKNOWLEDGMENTS

Willis Crumpler originated the basic concept of the Mass Properties Measurement System (MPMS) and Kedron R. Wolcott has led the theoretical analysis and data acquisition. R.J. McNulty contributed to its design and realization while Ron Remus guided its construction.

The authors gratefully acknowledge the support of the University of Central Florida faculty and staff along with the I-NET and NASA staffs whose diligence and kindness make the NASA Faculty Fellowship program at the Kennedy Space Center so efficient and productive. Particular thanks to Bill Jones and Todd Graham of NASA and James Spencer and Rich Bennett of I-NET.

1. INTRODUCTION

The Mass Properties Measurement System (MPMS), illustrated in Figure 1.1, consists of a serial kinematic mechanism with two intersecting revolute axes, z_0 and z_1, that intersect with fixed angle α_1. The joint angles and rates denoted by θ_1, θ_2 and $\dot{\theta}_1$, $\dot{\theta}_2$, respectively, turn about the respective joint axes. The angle θ_1 rolls the table about z_0 and will be called *tilt*.

The function of the MPMS is to measure the mass, center-of-gravity and second-order mass moments of an unknown mass placed on the turntable. The mass and center-of-gravity can be determined from statics measurements. The inertia tensor must be determined from the dynamics. Reference[1] provides a derivation of the MPMS dynamics equations.

In all the experimental work reported here, we have fixed the angle θ_2 at some value during a measurement. In other words, $\dot{\theta}_2 = 0$ and $\ddot{\theta}_2 = 0$ for all measurements performed in this study.

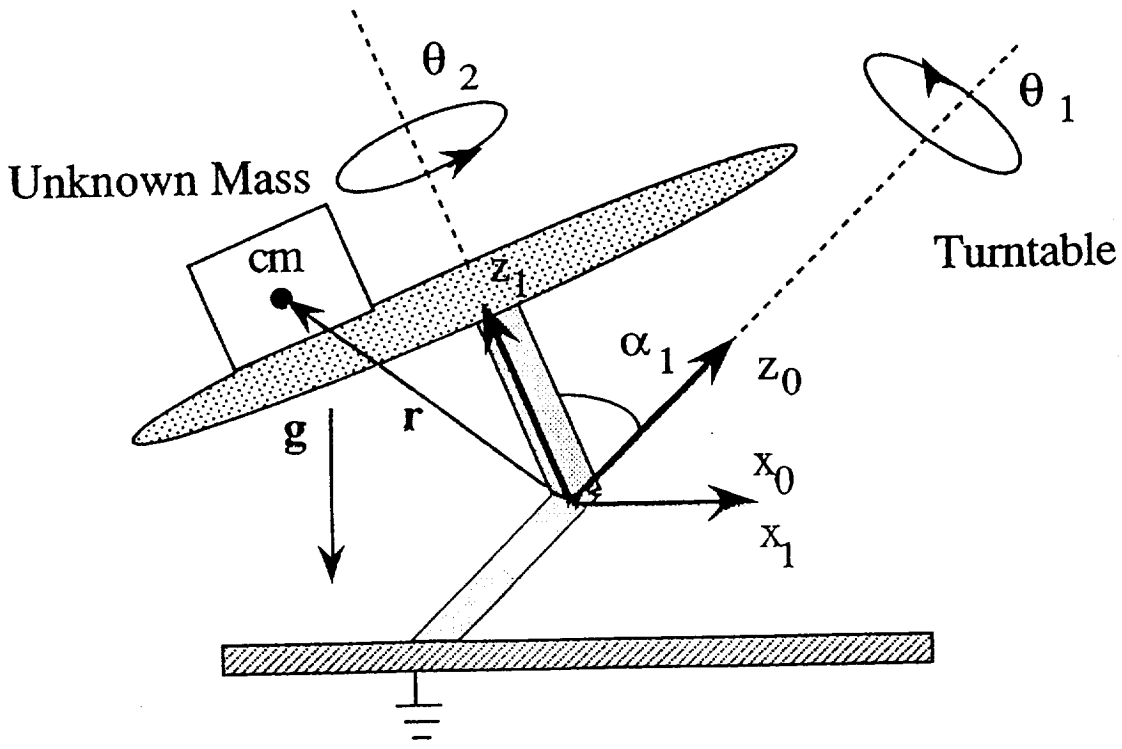

Figure 1.1 The Mass Properties Measurement System

MPMS Dynamics

The total torque τ_{total1} about the z_0-axis equals

$$\tau_{total1} = \tau_{KE1} + \tau_{PE1}. \tag{1-1}$$

According to (4-4a) in [1], with $\sigma_1 = \sin \alpha_1$, $\tau_1 = \cos \alpha_1$, $c_i = \cos \theta_i$, $s_i = \sin \theta_i$, $i = 1,2$, $r_1 = 0$, $r := r_2$ and $m := m_2$ in that equation, the potential energy related torque equals

$$\tau_{PE1} = m \sigma_1 g_c \{ r_x (c_1 c_2 - \tau_1 s_1 s_2) + r_y (-\tau_1 c_2 s_1 - c_1 s_2) + r_z \sigma_1 s_1 \}. \tag{1-2}$$

τ_{KE1} equals the torque associated with the motion of the system (refer to (4-29) in [1]),

$$\begin{aligned} \tau_{ke1} = \; & \ddot{\theta}_1 I_{T1} + I_{zz} \tau_1 (\ddot{\theta}_2 + \ddot{\theta}_1 \tau_1) + \sigma_1 \{ I_{yy} c_2 \sigma_1 (\ddot{\theta}_1 c_2 - 2 \dot{\theta}_1 \dot{\theta}_2 s_2) \\ & + I_{xx} \sigma_1 s_2 (2 \dot{\theta}_1 \dot{\theta}_2 c_2 + \ddot{\theta}_1 s_2) \\ & + I_{yz} (-\ddot{\theta}_2 c_2 - 2 \ddot{\theta}_1 c_2 \tau_1 + \dot{\theta}_2^2 s_2 + 2 \dot{\theta}_1 \dot{\theta}_2 \tau_1 s_2) \\ & + I_{xz} (-\dot{\theta}_2^2 c_2 - 2 \dot{\theta}_1 \dot{\theta}_2 c_2 \tau_1 - \ddot{\theta}_2 s_2 - 2 \ddot{\theta}_1 \tau_1 s_2) \\ & - I_{xy} \sigma_1 (2 \dot{\theta}_1 \dot{\theta}_2 c_{2\theta 2} + \ddot{\theta}_1 s_{2\theta 2}) \; \}. \end{aligned} \tag{1-3}$$

The term I_{T1} describes the inertia of the first link and the other inertia terms, I_{xx}, I_{yy}, I_{zz}, I_{xy}, I_{xz}, I_{yz} describe the inertia of the second link *plus* the unknown mass. Ultimately, to determine the inertia tensor of the unknown mass will require knowledge of the inertia terms of the MPMS links.

The analytical relation (1-2) provides the means for computing the center-of-gravity moment $\tau_g = m g r$ while (1-3) allows one to compute the inertia matrix I_2 formed by the combined mass of link two and the unknown mass.

MPMS Prototype

The first axis of the MPMS prototype aligns with the diagonal of a unit cube (Figure 1.3), hence, the angle the first axis makes to the floor equals

atan2($\sqrt{2}$,1) = 35.26°. The complement of this angle equals the twist α_1 = atan2(1,$\sqrt{2}$) ≈ 54.74°. The body attached frame z-axis initially aligns with the axis of θ_1. A rotation of the body by θ_2 = 120° will align the body attached frame x-axis to the first axis of the MPMS. Similarily, θ_2 = 240° will align the body attached frame y-axis to the first axis of the MPMS. This particular allignment permits determination of the diagonal entries of the inertia matrix by simply measuring the torque and position of the first axis. Computation of the off diagonal terms, however, requires θ_2 to be time varying and measured.

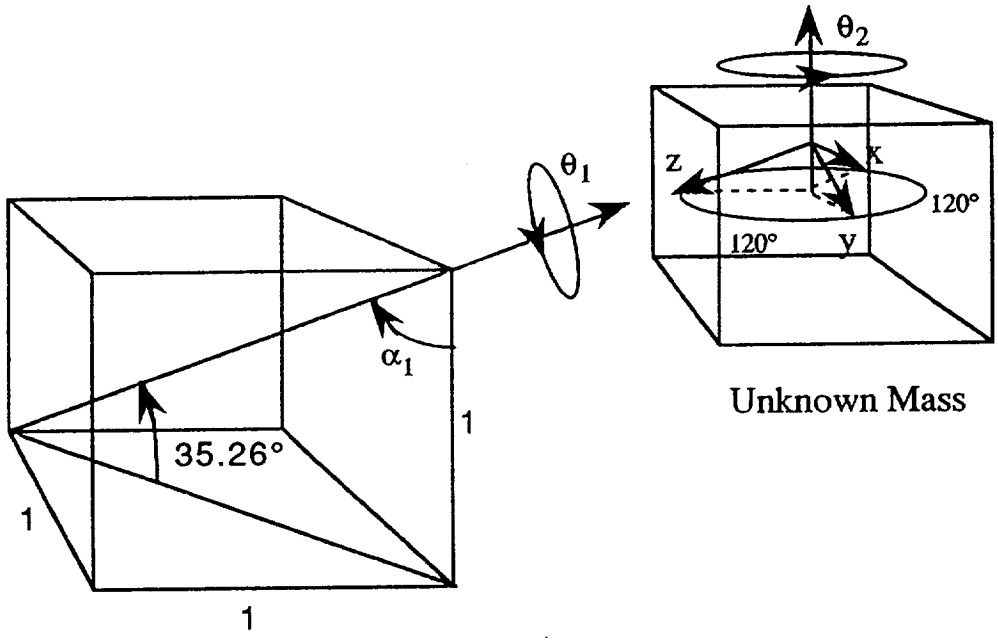

Figure 1.3 MPMS prototype with α_1 = atan2($\sqrt{2}$, 1) ≈ 54.74°.

2. COMPUTATION OF THE CENTER-OF-GRAVITY

To compute the center-of-gravity vector $r = \frac{\tau_g}{m\ g}$, the total mass m and gravitational constant g must be known. In the experiments to follow, we treat σ_1 m g r_x, σ_1 m g r_y and σ_1 m g r_z as the unknown terms and fix both axes. Measuring the reaction torque on the first axis for different configurations we can determine the actual values of r_x, r_y and r_z when the solutions are divided by σ_1 m g. Details of this procedure follow.

MPMS Statics Coefficient Matrix

The coefficients of $\sigma_1 m g r_x$, $\sigma_1 m g r_y$ and $\sigma_1 m g r_z$ in (1-2) equal

$$c_x := c_1 c_2 - \tau_1 s_1 s_2, \quad c_y := -\tau_1 c_2 s_1 - c_1 s_2 \text{ and } c_z := r_z \sigma_1 s_1 , \quad (2\text{-}1)$$

respectively. At $\theta_2 = \mu, \mu + 120°$ and $\mu + 240°$, where μ equals an arbitrary, but fixed, angle, the coefficients form the coefficient matrix

$$C_f = \begin{pmatrix} c_\mu c_1 - \tau_1 s_\mu s_1 & -c_1 s_\mu - c_\mu \tau_1 s_1 & \sigma_1 s_1 \\ -c_1 (c_\mu + \sqrt{3}\, s_\mu)/2 - \tau_1 (\sqrt{3}\, c_\mu - s_\mu) s_1/2 & -c_1 (\sqrt{3}\, c_\mu - s_\mu)/2 + \tau_1 (c_\mu + \sqrt{3}\, s_\mu) s_1/2 & \sigma_1 s_1 \\ c_1 (-c_\mu + \sqrt{3}\, s_\mu)/2 + \tau_1 (\sqrt{3}\, c_\mu + s_\mu) s_1/2 & c_1 (\sqrt{3}\, c_\mu + s_\mu)/2 + \tau_1 (c_\mu - \sqrt{3}\, s_\mu) s_1/2 & \sigma_1 s_1 \end{pmatrix} \quad (2\text{-}2)$$

A note about these choices for θ_2. Physically, the angles $\theta_2 = 0$, 120° and 240° were chosen to align axis one with three orthogonal axis F_b selected in the unknown mass. These choices of θ_2 permit calculating the diagonal entries of the inertia matrix, expressed in F_b coordinates, from torque and position measurements on the first axis alone. Serendipitously, these angles allows us to find an MPMS configuration for which the condition number of C_f equals one. In fact, any three angles separated by 120° will allow the MPMS to be configured such that a condition number of one can be achieved. Recall that a matrix C_f with a condition number of one guarantees the optimum numerical stability when inverting C_f.

By measuring the torque T_1 at joint one for each of the three angles selected for θ_2, we obtain the linear system of equations in the center-of-gravity unknowns,

$$\begin{pmatrix} T_{11} \\ T_{21} \\ T_{31} \end{pmatrix} = \sigma_1 m g C_f \begin{pmatrix} r_x \\ r_y \\ r_z \end{pmatrix} \quad (2\text{-}3)$$

Solving (2-3) produces

$$\begin{pmatrix} r_x \\ r_y \\ r_z \end{pmatrix} = \frac{1}{\sigma_1 \, m \, g} C_f^{-1} \begin{pmatrix} T_{11} \\ T_{21} \\ T_{31} \end{pmatrix} \qquad (2\text{-}4)$$

Two central issues arise: 1) For what configurations is C_f invertible and 2) how well conditioned is C_f for those situations where it is invertible?

The coefficient matrix C_f is invertible as long as

$$\det[C_f] = \frac{-3^{3/2}}{16} (6 + 2\, c_{2\alpha_1} - c_{2(\alpha_1 - \theta_1)} + 2\, c_{2\theta_1} - c_{2(\alpha_1 + \theta_1)})\, \sigma_1\, s_1 \neq 0. \qquad (2\text{-}5a)$$

Notice that the determinant does not depend upon the initial angle μ selected for θ_2 as long as the angles differ by 120°. The determinant of the coefficient matrix can also be written simply as

$$\det[C_f] = \frac{-3^{3/2}}{2} (1 - \sigma_1^{\,2}\, s_1^{\,2})\, \sigma_1\, s_1 \,, \qquad (2\text{-}5b)$$

by using the not so obvious, but directly verifiable identity

$$6 + 2\, c_{2\alpha_1} - c_{2(\alpha_1 - \theta_1)} + 2\, c_{2\theta_1} - c_{2(\alpha_1 + \theta_1)} = 8\,(1 - \sigma_1^{\,2}\, s_1^{\,2}). \qquad (2\text{-}6)$$

The condition $\sigma_1\, s_1 \neq 0$ means that the angle θ_1 and the twist α_1 between the two axes cannot be zero or a multiple of π. These design constraints make physical sense. Positioning the turntable at three different angles with $\theta_1 = 0$ will not change the z-component of the center-of-mass, and, therefore, cannot provide information about r_z. The same observation applies to the case where the twist α_1 equals zero.

The term $(1 - \sigma_1^{\,2}\, s_1^{\,2}) = 0$ when $\alpha_1 = \theta_1 = \pm \frac{1}{2}\pi$. The MPMS with this physical configuration can only measure r_z.

Design Criterion

The MPMS configuration and structure must satisfy $\sigma_1\, s_1 \neq 1$ and $\sigma_1\, s_1 \neq 0$. *In particular, the MPMS must have a non-zero twist* α_1 *between the two axes.*

In the course of experimentation, sometimes the computed solutions based on the data varied wildly. Analysis of the causes revealed that one error source was the ill-conditioning of the numerical inversion of C_f.

Condition Number of the MPMS Statics Coefficient Matrix

The condition number c_n for C_f equals

$$c_n = \sqrt{\left|\frac{\lambda_{max}}{\lambda_{min}}\right|} \tag{2-7}$$

where λ_{max} and λ_{min} are the maximum and minimum eigenvalues, respectively, of $C_f^\tau C_f$. We now calculate the condition number c_n of C_f as a function of the twist α_1 between the shafts and θ_1, the angle of the first shaft. This will allow us to determine the angle settings for θ_1 which

Using (2-2), direct computation yields

$$C_f^\tau C_f = \begin{pmatrix} \lambda_1 & 0 & 0 \\ 0 & \lambda_2 & 0 \\ 0 & 0 & \lambda_3 \end{pmatrix},$$

where $\lambda_1, \lambda_2, \lambda_3$ clearly equal eigenvalues of $C_f^\tau C_f$ and compute to

$$\lambda_1 = \frac{3}{16}(6 + 2\, c_{2\alpha_1} - c_{2(\alpha_1 - \theta_1)} + 2\, c_{2\theta_1} - c_{2(\alpha_1 + \theta_1)}, \tag{2-8a}$$

$$\lambda_2 = \frac{3}{16}(6 + 2\, c_{2\alpha_1} - c_{2(\alpha_1 - \theta_1)} + 2\, c_{2\theta_1} - c_{2(\alpha_1 + \theta_1)}, \tag{2-8b}$$

$$\lambda_3 = 3\, \sigma_1^{\,2}\, s_1^{\,2}, \tag{2-8c}$$

and do not depend upon the arbitrary angle μ added to 0°, 120° and 240° to θ_2.

Define $\gamma = \sqrt{\left|\frac{\lambda_1}{\lambda_3}\right|}$. Applying (2-6) produces the simple expression

$$\gamma := \sqrt{\frac{1 - \sigma_1^{\,2}\, s_1^{\,2}}{2\,\sigma_1^{\,2}\, s_1^{\,2}}}\,. \tag{2-9}$$

Whenever $\lambda_3 \le \lambda_1$, the condition number c_n of C_f equals γ. On the other hand, if $\lambda_1 < \lambda_3$, the condition number c_n of C_f equals $1/\gamma$,

$$\textit{if}\ \ \gamma < 1, \textit{then}\ \ c_n = 1/\gamma\ \ \textit{else}\ \ c_n = \gamma. \tag{2-10}$$

Selecting the Twist and Tilt to Optimize Condition Number

A plot of c_n versus θ_1 appears in Figure 2.1 for $\alpha_1 = \text{atan2}(1,\sqrt{2}) \approx 54.74°$, the angle employed in the prototype (Figure 1.3). Details of the W-shaped portion of the curve is illustrated in Figure 2.2.

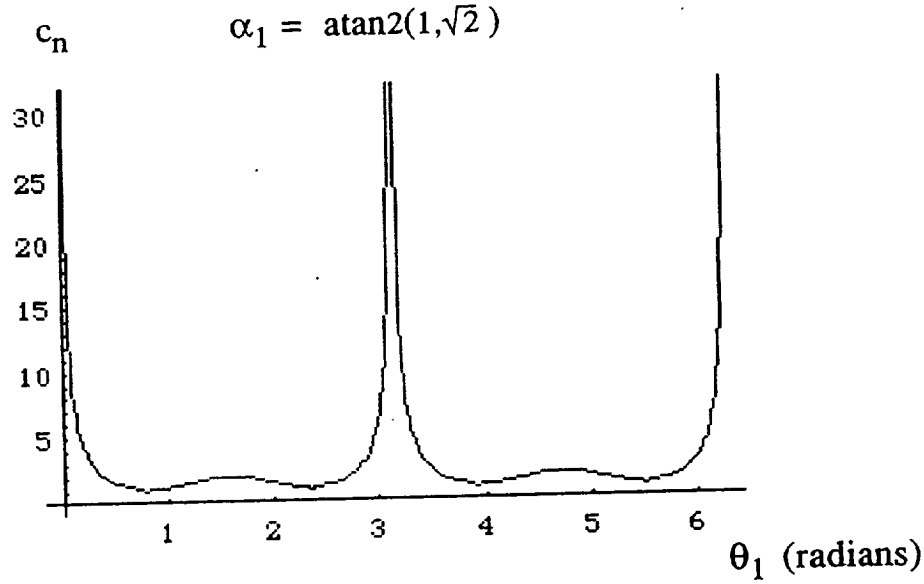

Figure 2.1 The condition number c_n of the coefficient matrix C_f vs. the angle θ_1 of the first shaft for $\alpha_1 = \text{atan2}(\sqrt{2}, 1)$.

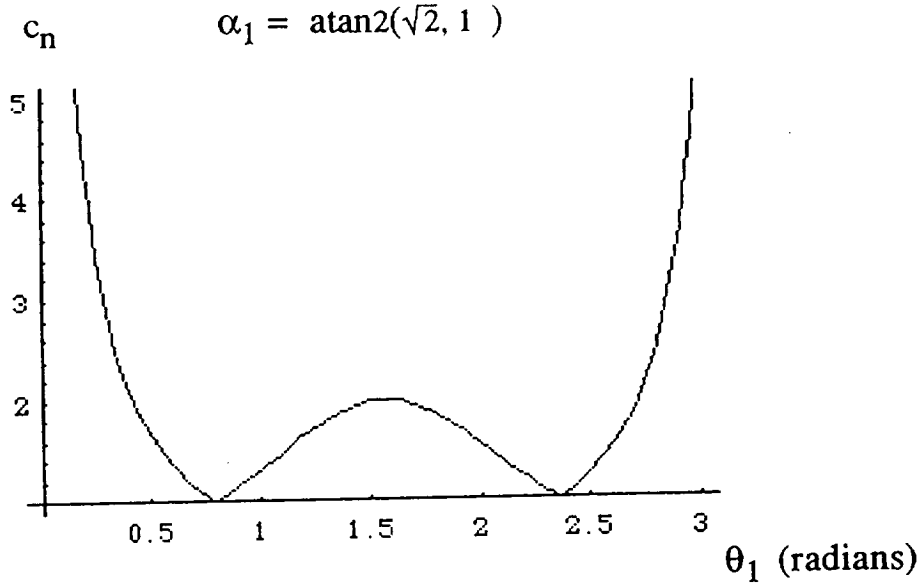

Figure 2.2 Details of the condition number $\alpha_1 = \text{atan2}(\sqrt{2}, 1)$.

The condition number $c_n = 1$, its optimum value, at that value of θ_1 for which $c_n - 1 = 0$. This occurs at $\theta_{1opt} = 0.7853981633974484\ 180/\pi = 45°$.

A plot of c_n versus θ_1 appears in Figure 2.3 for $\alpha_1 = \pi/2$. Details of one period of the curve is illustrated in Figure 2.4.

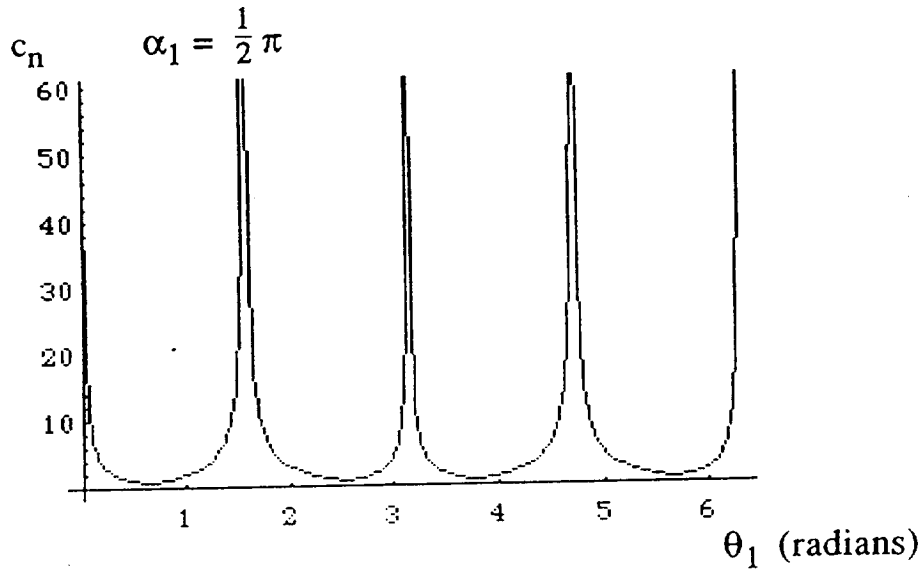

Figure 2.3 The condition number c_n of the coefficient matrix C_f vs the angle θ_1 of the first shaft for $\alpha_1 = \frac{1}{2}\pi$.

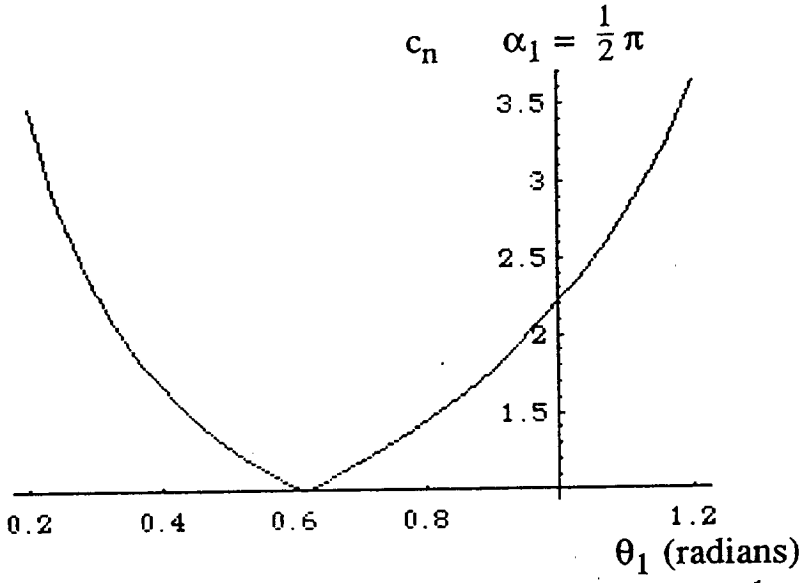

Figure 2.4 Details of the condition number for $\alpha_1 = \frac{1}{2}\pi$.

The condition number $c_n = 1$ at that value of θ_1 for which $c_n - 1 = 0$. This occurs at

$$\theta_{1opt} = 0.6154797086703873\ 180/\pi = 35.2644 = \alpha_1 = \text{atan2}(\sqrt{2}, 1).$$

MPMS Configurations with Condition Number of One

A general plot of the condition number (Figure 2.5) illustrates the nature of the condition number when the three angles selected for θ_2 split the circle into three 120° arcs. The plot has been truncated at $c_n = 5$ to display the important characteristics of the function.

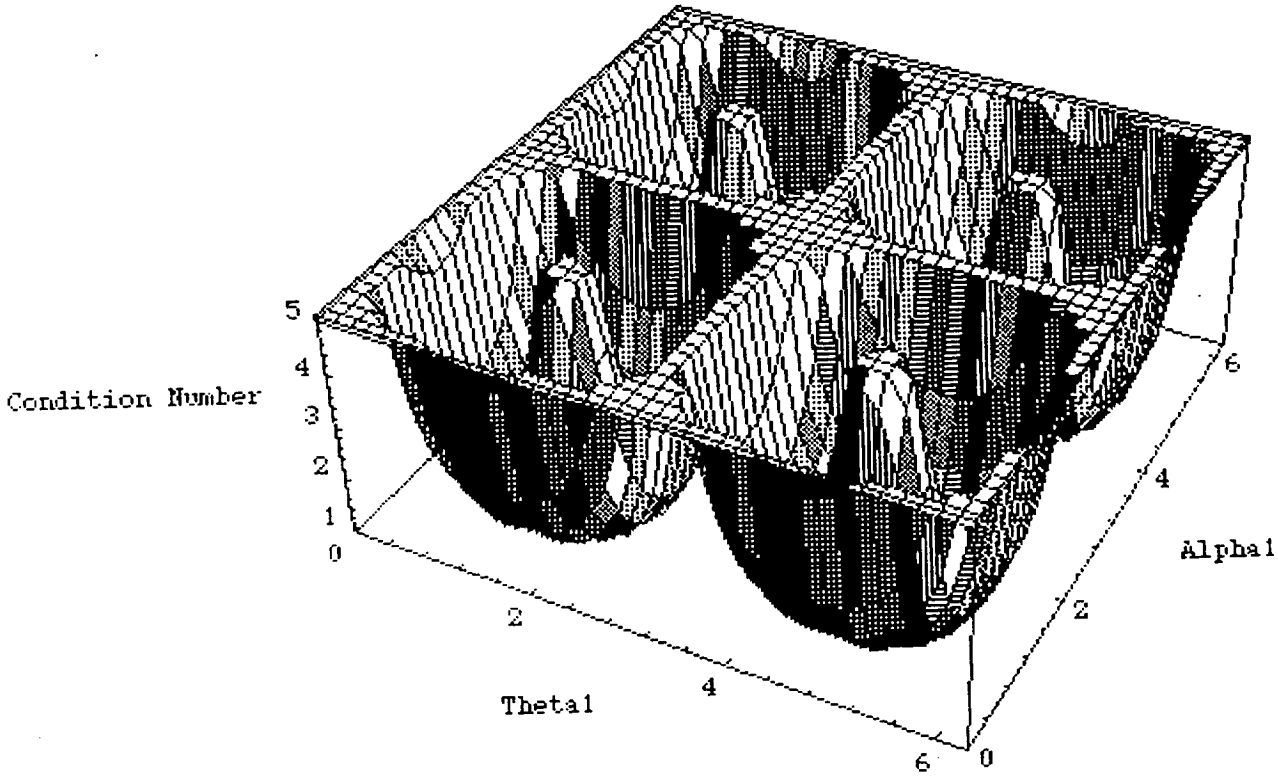

Figure 2.5 Plot of the condition number, clipped at c_n=5, as a function of θ_1 and the angle α_1 between the first and second axis.

The condition number plotted in Figure 2.5 applies for any three angles chosen for θ_2 which are separated by 120°. The function c_n is symmetric in θ_1 and α_1 and has period of π along each axis. Figure 2.6 illustrates a single quadrant of Figure 2.5 in more detail and Figure 2.7 depicts an overhead view.

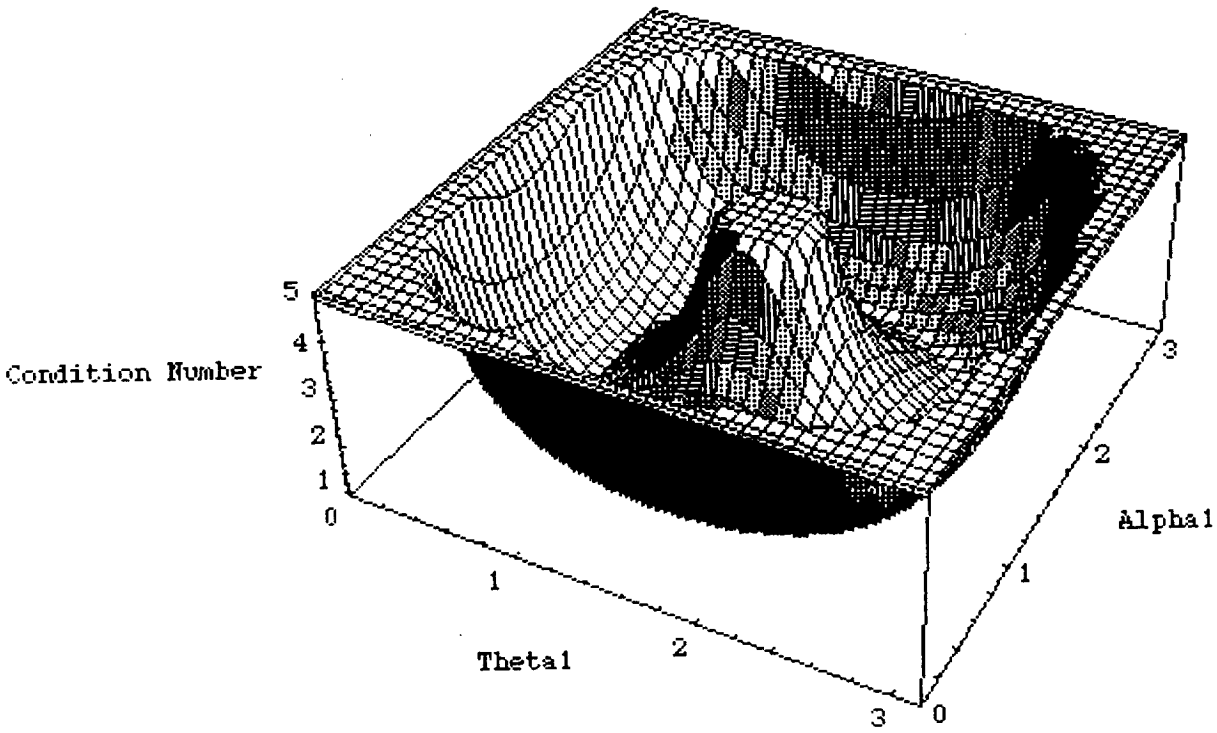

Figure 2.6 Plot of one quadrant of the condition number clipped at c_n=5.

When the condition number is one, all the eigenvalues of $C_f^{\tau} C_f$ must equal one. In particular, for $c_n = 1$, (2-9) implies

$$\lambda_3 = 3\,\sigma_1^{\,2}\, s_1^{\,2} = 3\ \sin^2(\alpha_1)\ \sin^2(\theta_1) = 1. \qquad (2\text{-}11)$$

Furthermore, if $\lambda_3 = 1$, (2-9) and (2-8) easily proves that $\lambda_1 = \lambda_2 = 1$ and, hence, $c_n = 1$. Consequently, (2-11) provides a design equation for the MPMS . For example, the minimum tilt θ_1 possible for $c_n = 1$ occurs when $\sigma_1^{\,2} = 1$, i.e., $\alpha_1 = \pm 90°$. The minimum angle θ_1 must, therefore satisfy $s_1^{\,2} = \frac{1}{3}$, yielding $\theta_1 = \pm 35.26°$.

The crease at the bottom of the well in Figure 2.7 depicts the curve (2-11) on which the condition number of the coefficient matrix equals one.

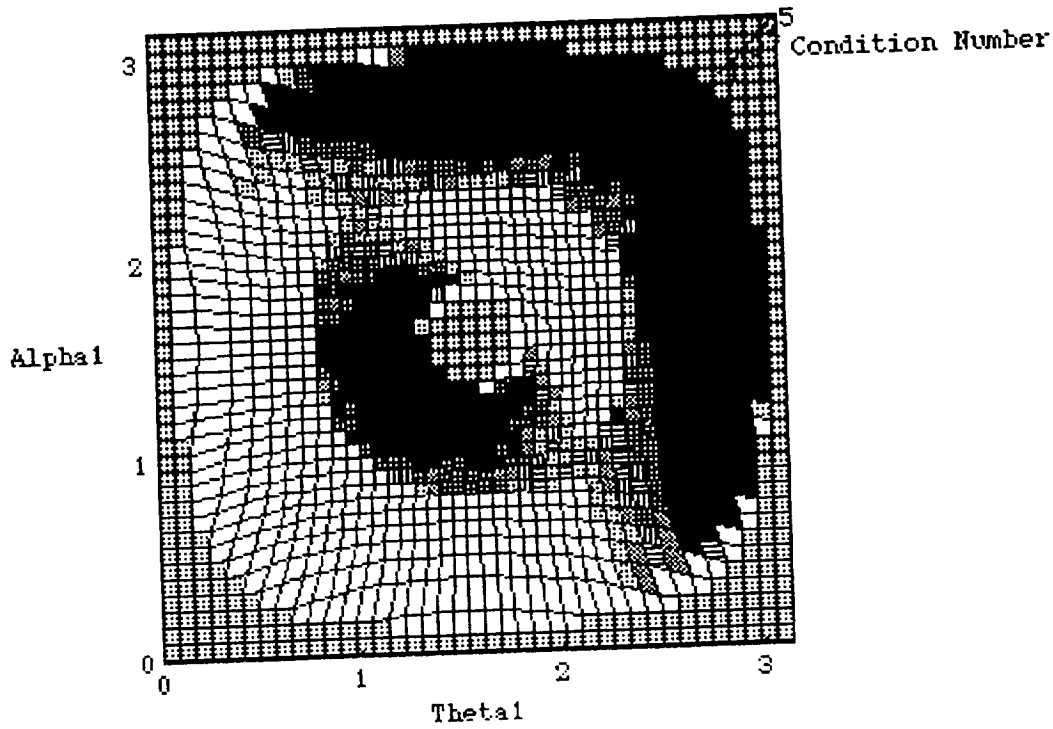

Figure 2.6 Top view of one quadrant of the condition number clipped at c_n=5.

3. STATICS MEASUREMENTS

Another source of error discovered in MPMS center-of-gravity measurements was the absolute accuracy of the torque sensor attached to $\mathbf{z}_0$. The torque sensors was rated 1% of full-scale rating of approximately 1900 in-lb. Measured torques of 40 in-lb could be off as much as 50%. Furthermore, if the condition number of the coefficient matrix where as little as 4, for example, with a twist $\alpha_1 = 54.73°$ and a tilt of $\theta_1 = 25.24°$, the error in the values for the center-of-gravity components could be as large as 100%. In fact, it was just such large errors that prompted us to look at the conditioning of the coefficient matrix and seek twist, tilt and turntable angles that would yield a condition number of one.

Statics Measurement Criterion

The three turntable angles (θ_2) should trisect the circle and the tilt angle θ_1 should be selected to satisfy (2-11) for a given α_1.

Tilt Axis Torsion

The dynamics measurements later will require oscillating the tilt axis at some prescribed frequency. Any significant torsion spring action of the tilt axis would affect the dynamics measurement. Essentially, we wanted to determine the MPMS natural frequency to ascertain whether the tilt axis torsion would have to be modeled in the dynamics. The prototype MPMS, upon which all experiments were performed, possesses the twist angle $\alpha_1 = 54.73°$.

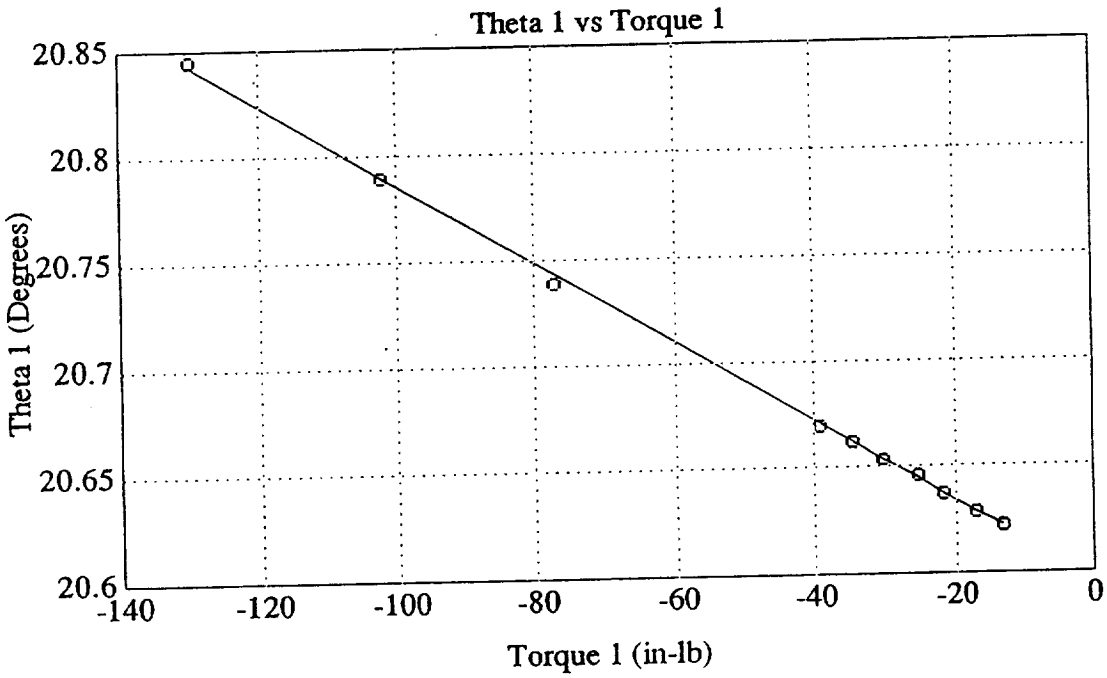

Figure 3.1 Compliance of the tilt axis: $\delta\theta_1 = (-0.0019°/\text{in-lb})\ \tau_1 + 20.5965°$

Figure 3.1 depicts the relationship between the angular deflection $\delta\theta_1$ of the tilt axis as a function of the torque τ_1 exerted about that axis. The experimental compliance c = 1/k of the tilt axis equals c = 0.0019°/in-lb. Assuming frictionless operation, the natural frequency of the MPMS with the second joint fixed approximately equals 16 Hz for a 50 lb force, 4 in from the first axis,

$$f_n = \sqrt{\frac{k}{I_m}} \approx \sqrt{\frac{32.2*12}{0.0019*50*4^2}} \approx 16 \text{ Hz.} \qquad (3\text{-}1)$$

In order to ignore the tilt axis torsion spring effect in the dynamics measurements, we should oscillate the table well below the resonant frequency of the second link and payload. A payload 9 times larger than the 50 lb force, however, would produce a resonant frequency of about 5.3 Hz. Such a low resonance would probably require modelling the shaft torsion for the dynamics measurements.

Center-of-Gravity Measurements

The minimum-norm, least-squares values for the first mass-moments of the turntable, plus an unknown mass placed on the turntable, yielded a first-mass moment vector of m g **r** ≈ [160 -41 284] (in-lb). The vector m g **r** was calculated from the average values of 3000 torque samples per experiment, taken from 30 experiments. The 30 experiments consisted of permutations of 10 measurements taken at each of the three MPMS configurations $\{(\theta_1 , \theta_2)\} = \{$ (35°,0) , (-35°,120°), (-35°,240°) $\}$.

Since the torque sensor used in the prototype MPMS generated absolute errors of 19 in-lbs, small, first-order mass moments measurement were exceptionally error prone. Figure 3.2 illustrates this point quite clearly. The three curves indicate the error of each experiment about the solution m g **r** ≈ [160 -41 284] (in-lb). The "blue" plot (the one that starts in the upper left-hand corner of the diagram) indicates the most error in measurement. Although 19 in-lb almost equal 50% of the measured y-axis first mass-moment of -41 in-lb, the huge number of samples over which averages were computed produced consistent results within ±6%. The larger values of the x-axis and z-axis first mass-moments produced more accurate readings; within ±1% for m g r_x (the "red" plot has a negative relative error for the first experiment) and within ±0.5% for m g r_z ("green" plot). These results are consistent with the fact that the absolute error of 19 in-lb has much less effect on the larger torque measurements.

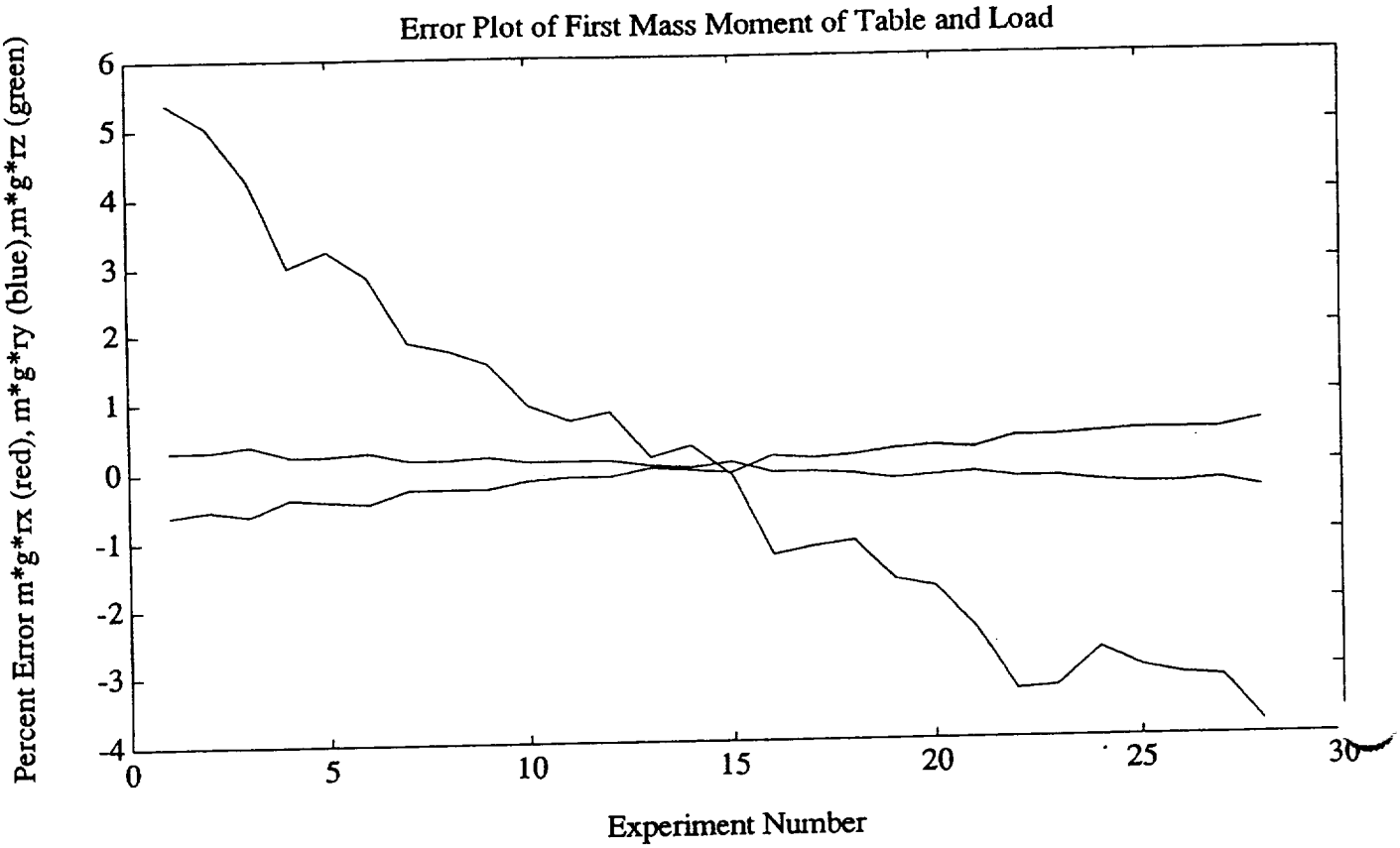

Figure 3.2 Percent error about mean of first order mass moment. At the far left the top plot is "blue", the middle plot "green" and the lower plot "red".

4. DYNAMICS MEASUREMENTS

The dynamics equation (1-3) for α_1= 54.73° ($\sigma_1 = \sqrt{\frac{2}{3}}$, $\tau_1 = \frac{1}{\sqrt{3}}$), $\ddot{\theta}_2 = 0$, $\dot{\theta}_2 =$ 0, produces

$$\tau_{kel} = \{I_{T1} + I_m\}\ \ddot{\theta}_1, \qquad (4\text{-}1)$$

where

$$I_m := \frac{1}{3}\left(2\, I_{xx}\, s_2^{\,2} + 2\, I_{yy}\, c_2^{\,2} + I_{zz} - 2\, I_{xy}\, s_{2\theta 2} - 2^{3/2}\, I_{xz}\, s_2 - 2^{3/2}\, I_{yz}\, c_2 \right)\} \ddot{\theta}_1 . \qquad (4\text{-}2)$$

To test the MPMS prototype, we measured the angular position θ_1 and total torque $\tau_{total1} = \tau_{KE1} + \tau_{PE1}$ at joint one versus time in order to calculate the total inertia seen by the first joint,

$$\{I_{T1} + I_m\} = \frac{\tau_{total1} - \tau_{PE1}}{\ddot{\theta}_1} \quad . \tag{4-3}$$

The gravity term τ_{PE1} exceeds τ_{KE1} by a factor from 10 to 60 , hence, the torque difference $\tau_{total1} - \tau_{PE1}$ will be quite small. Subtracting two nearly equal numbers produces large numerical errors. Initial experiments proved this to be a significant problem. To eliminate it we balanced the unknown mass so as to make the gravity torque $\tau_{PE1} \approx 0$. We then manually oscillated the second link and the unknown mass point at about 8.7 Hz about the $\tau_{PE1} = 0$ and measured the resultant torque and angular position.

We compute the angular acceleration $\ddot{\theta}_1$ from θ_1 by the central difference formula [1],

$$\ddot{\theta}_1(t_0) = \frac{-\theta_1(t_2) + 16\,\theta_1(t_1) - 30\,\theta_1(t_0) + 16\,\theta_1(t_{-1}) - \theta_1(t_{-2})}{12\,h^2} + O(h^4). \tag{4-4}$$

where $h = t_i - t_{i-1} = 4\ ms$ and $O(h^4)$ indicates errors on the order of h^4.

Figures 4.1 and 4.2 depict typical position and torque signals, respectively, for a given experiment. The 12 in-lb absolute accuracy of the torque sensor used in the prototype resulted in large instantaneous errors when measuring the small inertia

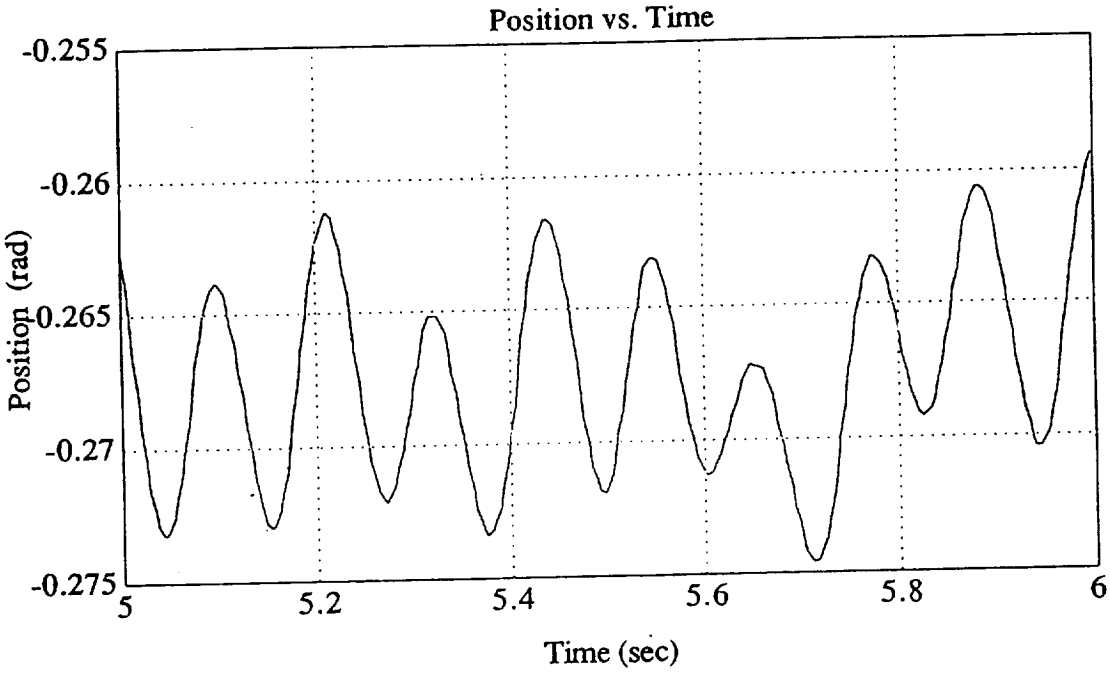

Figure 4.1 A plot of θ_1 vs time.

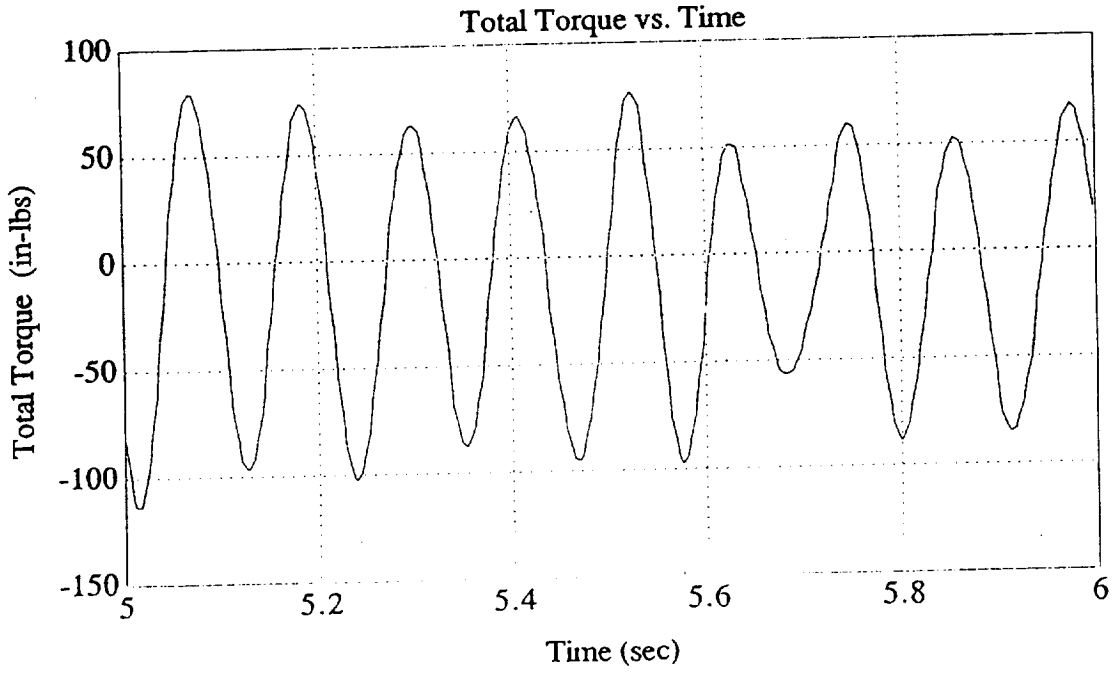

Figure 4.2 A plot of τ_{total1} vs time.

torques. The mean of the absolute value of the torque $\overline{|\tau_{kel}|}$ and position derived angular acceleration $\overline{|\ddot{\theta}_1|}$ were computed for each experiment consisting of 5000 points. The ratio of these values were then taken as the estimate for the measured inertia $\{I_{T1} + I_m\}$,

$$\{I_{T1} + I_m\} \approx \frac{\overline{|\tau_{kel}|}}{\overline{|\ddot{\theta}_1|}} \tag{4-5}$$

Figure 4.3 indicates the inertia measurement percent error for 10 different experiments with respect to their mean value. The error is bounded ±10% about a mean of 4.34 in-lb-s^2. These large error bounds can plausibly be attributed to the torque sensor sensitivity. The measured torque values in Figure 4.2 were less than 10% full scale, hence, the torque sensor, which is rated 1% accuracy at full scale, produces approximately 10% error in the measurements.

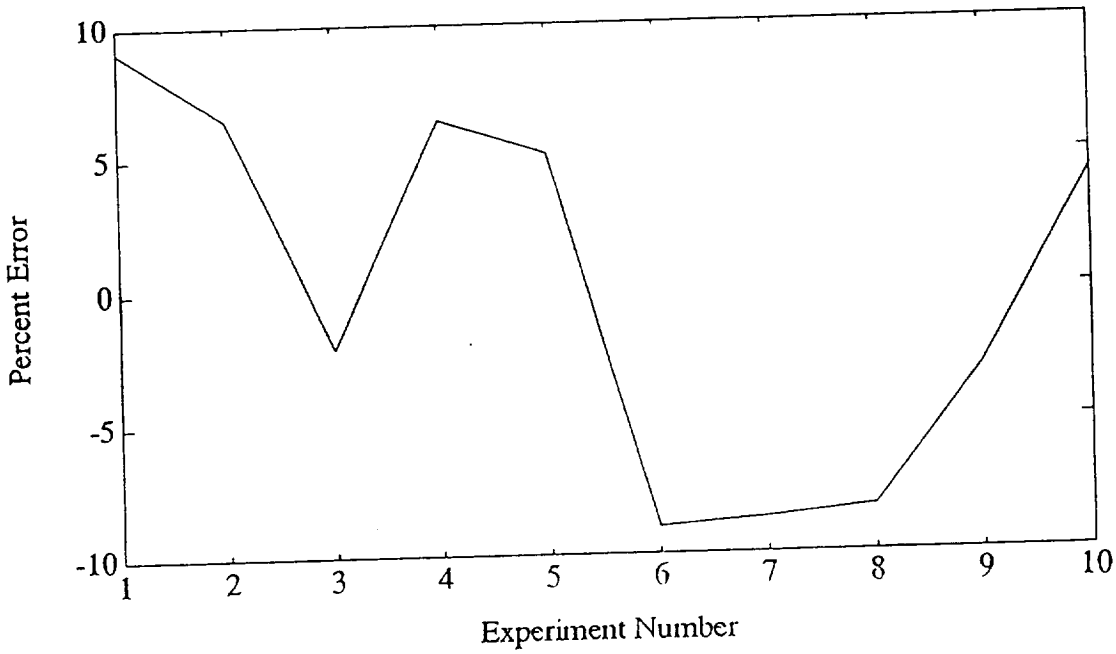

Figure 4.3 Percent Error in Inertia about Mean of 4.34 in-lb-s^2

5. OBSERVATIONS OF MPMS PERFORMANCE

With single torque sensor and position sensor, one can measure the center-of-gravity and the moments of inertia about three orthogonal axes. However, one must minimally move and measure the velocity and acceleration of the second axes in order to obtain the full inertia tensor. These facts were established in [1].

To obtain accurate center-of-gravity measurements one should select MPMS configurations where the condition number c_n of the coefficient matrix equals one. In other words, the choice of angles selected for measuring the center-of-gravity matter significantly. A poor choice of angles can multiply the measured error by a factor $1 \leq c_n < \infty$. This explained why, in some of our earlier experiments the errors where 600%.

Torque readings for both statics and dynamics measurements at the lower limit of the torque sensor resolution also had significant impact on the measurement reliability. The location of the center-of-gravity of the unknown mass affects the size of the torque readings. This suggests placing the mass center away from the z_1-axis in order to drive the force sensor harder and produce more accurate results. Taking these details into consideration center-of-gravity measurements we made highly repeatable measurements (±0.4%) for a specific configuration and setup.

Gravity torque dominates dynamics measurements and extreme measures must be taken to minimize its affects. Dynamics measurements were made at a balance point of the turntable using "high" frequency oscillations (≈ 8 Hz). The combination of the smaller gravity terms about the balance point and the increased inertia effects for high speed oscillations enabled us to more accurately measure the much smaller inertial terms than would otherwise be possible. Higher frequency oscillation are precluded because of the MPMS resonance near 16 Hz . Dynamics measurements were repeatable (±3.0%) for a given configuration and setup and stayed within ±10.0%, even though the measurements were near the lower resolution limit of the torque sensor.

Stiction and friction also appear to play an important role in inertia measurements on the MPMS. Stiction was particularly noticeable when balancing the turntable. These effects were not modeled in this effort, but should be taken into account in a later prototype.

6. RECOMMENDATIONS

In [1] it was recommended to make the twist $\alpha_1 = 90°$. Further support for this design change arises in the condition number c_n analysis provided earlier. That analysis proved that the minimum tilt angle of 35.26° for $c_n = 1$ can only be achieved when $\alpha_1 = 90°$. By comparison $\alpha_1 = 5.74°$ in the current prototype and the tilt angle must be 45° in order for $c_n = 1$.

At this point the limitations of the current prototype appear to be well understood and further experimentation is contraindicated. If management decides to continue with the MPMS concept, the follow-on prototype will require some modificatins to correct the discovered problems with the first model.

The prototype MPMS permitted only manual actuation of joint one. A second generation MPMS should :

1. Include automatic operation of both axes,
2. Match torque sensor with expected loads,
3. Utilize low friction bearings,
4. Add a position sensor on the second axis,
5. Incorporate a torque sensor on the second joint,
6. Explore concept with potential customers

7. CONCLUSIONS

Theoretical results verify the MPMS concept in principle, but experimental results indicate several engineering limitations in the current implementation. In particular, the torque sensor must be able to accurately measure a broad range of values. The gravity terms dominate the dynamics and this fact makes it difficult to obtain good inertial measurements.

To obtain the optimum performance from the MPMS when measuring center-of-gravity:

1. Place the unknown mass's center-of-gravity away from the turntable center.

2. Measure the center-of-gravity every 120° turn of the turntable.

3. Tilt the turntable to the optimum angle to produce a condition number of one for the coefficient matrix.

When measuring inertia :

4. Place the unknown mass so that the turntable axis passes through its center-of-gravity.

5. Oscillate the turntable well below the resonant frequency of the MPMS about the null gravity torque configuration .

Items 1 and 4 clearly compete with one another. Placement issues have not been addressed here and would need further exploration should the MPMS project proceed.

REFERENCES

1. Doty, Keith L,1993, "Mass Properties Measurement System Dynamics", Kennedy Space Center, NASA Faculty Fellow internal report.

2. Gerald, C.F. and Wheatley, P.O., "Applied Numerical Analysis", Addison Wesley,1984, pp.243.